First publ. in: Applied Physics A 78 (2004), pp. 471-475

Light-emitting silicon *pn* diodes

T. DEKORSY✉
J.M. SUN
W. SKORUPA
B. SCHMIDT
M. HELM

Institut für Ionenstrahlphysik und Materialforschung, Forschungszentrum Rossendorf, Postfach 510119, 01314 Dresden, Germany

ABSTRACT We report on the electrical and optical characteristics of silicon light-emitting *pn* diodes. The diodes are prepared by ion implantation of boron at high doses and subsequent high-temperature annealing. Under forward bias, the diodes emit infrared electroluminescence closely below the band gap of bulk Si. We present a rate-equation model for bound excitons, free excitons and free carriers which successfully describes the electrical and optical behaviour of the diodes at low temperatures. Especially, an electrical bistability observed below 50 K is shown to be based on the interplay of bound excitons, free excitons and free carriers in the active area of the diodes. The ionisation of bound excitons is the origin of an improved electroluminescence from the diodes at higher lattice temperatures.

PACS 78.60.Fi; 78.55.Ap; 71.35.-y; 71.55.Cn

1 Introduction

Silicon – the key material of microelectronics – is an inherently bad light emitter due to its indirect fundamental band gap. Disregarding this fundamental drawback there are continuously strong efforts ongoing to tailor light emitters from silicon or from material combinations that are fully compatible with the ultra large scale integration (ULSI) technology employed for silicon microelectronics. One driving force for these efforts is to overcome the interconnect bottleneck of future integrated circuits: as the integration density is increased, electrical interchip and on-chip connects represent a formidable problem concerning space, bandwidth and power requirements. For the year 2010 an electrical interconnect pitch of 140 nm and a total length of interconnects per chip of 20 km are predicted, which would lead to a power dissipation of more than 60% of the total power consumption of the chip by the interconnects only [1]. Optical interconnects could be the solution towards this problem, as photonic circuits could in principle outperform electronic circuits for this purpose in many ways. One pathway are hybrid solutions by exploiting the third spatial dimension for interconnects with vertical-emitting III–V-based high-efficiency diodes or lasers. These exhibit extremely good performances concerning power efficiency ($> 50\%$) and modulation speed in the high-GHz range. However, since the technology for hybridisation such as solder bumps or wafer bonding is troublesome, a solution more compatible with ULSI technology is highly desired.

✉ Fax: +49-351/2603285, E-mail: t.dekorsy@fz-rossendorf.de

In the past years several routes were followed to realise silicon-based light emitters [2–7]. The realisation of an electrically driven device would represent an important technological breakthrough [8]. The main routes pursued so far with relevance for optical interconnects are based on (i) porous silicon emitting in the infrared to visible spectral range depending on its processing history [9–12], (ii) Si nanocrystals in silicon dioxide emitting in the red to blue spectral range [3, 13, 14], (iii) erbium (Er^{3+})-doped silicon [15–18] or Er^{3+} in SiO_2 sensitised by Si nanoclusters [7] emitting at 1.5 μm corresponding to a 4f intra-shell transition of the Er^{3+} ions, (iv) SiGe heterostructures and quantum dots exploring effects of quantum confinement [19–22] and (v) band-to-band recombination in Si *pn* diodes [4–6, 23]. In this paper we focus on the last approach, since it is fully compatible with standard ULSI process technology.

The diodes under investigation are prepared by high-dose boron (B^+) implantation into *n*-doped Si substrates for formation of a *pn* junction. High-temperature annealing leads to the reduction of the implantation damage. At the high doses used for implantation, during annealing the B concentration exceeds locally the solubility limit for B in Si. As a result, locally high boron concentrations are present in the *pn* junction. Bound excitons are formed in this region of high B concentrations with binding energies depending on the local strain environment. We investigate the electrical and optical properties of these light-emitting *pn* diodes. We compare the experimental results to calculations based on a rate-equation model for excitons and free carriers. It is shown that the model quantitatively accounts for an experimentally observed bistability in the *I–V* characteristics of the diodes [24] as well as the temperature dependence of the luminescence intensity from the diodes. The excellent agreement between theory and experiment points out the role of excitons in the optical and electrical characteristics of the diodes.

2 Rate-equation model

We consider a semiconductor *pn* junction containing excitonic traps introduced by doping or intrinsic defects. Electrons and holes are injected from the *n* and *p* layers, respectively, to the *pn* junction under forward bias; excitons are

formed by Coulomb attraction between a positively charged hole and a negatively charged electron in the neutral-charged region of the *pn* diode. Free excitons and bound excitons are distinguished: the free excitons can diffuse freely and are dissociated into free electrons and holes by the built-in internal electric field of the *pn* diode, as has been discussed for silicon solar cells [25, 26]. Therefore, free excitons partially contribute to the conductivity in a *pn*-junction diode [27]. Bound excitons are formed from free excitons and carriers bound to defects or isoelectronic excitonic traps. Since the bound excitons cannot move freely in the semiconductor, they do not directly contribute to the conductivity. The influence of bound excitons on the conductivity is based on the trapping and detrapping of free excitons or free electron–hole pairs during their formation, ionisation and radiative annihilation [28, 29]. Therefore, the conductivity of the semiconductor will be influenced indirectly through the density of bound excitons and the interactions among bound excitons, free excitons and free carriers. Figure 1 shows a schematic diagram of a three-level model containing these three species. Free carriers and free excitons are treated as a single level, since the binding energy is very small and the Coulomb attraction is screened at higher injection currents. In Fig. 1, G denotes the generation rate of free excitons and free carriers; n, n_0, n_t and N_t are the free-carrier density, the free-exciton density, the bound-exciton density and the excitonic-trap density, respectively; c_t and e_t are the probability of the formation of bound excitons and thermal dissociation probabilities of bound excitons into free excitons and free carriers, respectively and W_t and W_0 are the total recombination probability of bound and free excitons, which are equal to the sum of the radiative and nonradiative transition probabilities $W_{rt} + W_{nt}$ and $W_{r0} + W_{n0}$, respectively.

An equivalent circuit of the *pn*-junction diode is also shown in Fig. 1. The *pn* diode is treated as an ideal diode with a series resistance $R_s = R_c + R_b$ consisting of two parts: one is a constant small series resistance R_c from the conductivity of the substrate, ohmic contacts, etc.; the other part is the sum of the variable resistance R_b of n and p layers, which is determined mainly by the free-carrier density. In order to simplify the theoretical model, the free excitons and free carriers are treated as one broad energy level, since the binding energy of free excitons is very small and dissociation of free excitons by the electric field in the light-emitting area will be strong. The temperature dependence of the transition rates is accounted for by setting the de-trapping probability of the bound excitons as $e_t = e_{t0} \exp(-E_a/kT)$, where e_{t0} is a constant and E_a is the thermal activation energy of the bound excitons.

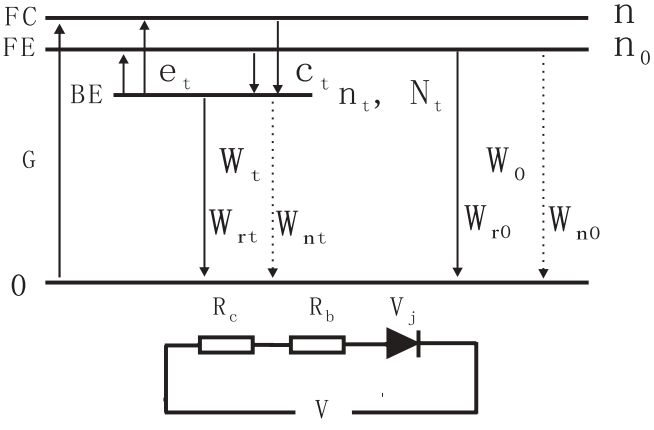

FIGURE 1 Model for free carriers (FC), free excitons (FE) and bound excitons (BE) used for the solution of rate equations describing the electrical and optical characteristics of a Si *pn* diode. In the *lower part* the equivalent circuit of the *pn* diode is shown

The rate equations of the systems consisting of free carriers/excitons and bound excitons are expressed as follows [30]:

$$\frac{\mathrm{d}(n_0+n)}{\mathrm{d}t} = G + n_t e_t - (n_0+n)c_t\left(1-\frac{n_t}{N_t}\right) - (n_0+n)W_0, \tag{1}$$

$$\frac{n_t}{\mathrm{d}t} = -n_t e_t + (n_0+n)c_t\left(1-\frac{n_t}{N_t}\right) - n_t W_t\,. \tag{2}$$

Under a steady-state condition where $\mathrm{d}n_0/\mathrm{d}t = 0$ and $\mathrm{d}n_t/\mathrm{d}t = 0$, i.e. in the current-controlled mode, the total generation rate is proportional to the injection-current density J. Therefore, we can derive the valid positive-value solutions by solving (1) and (2). The general solution for the sum of the free-exciton and free-carrier densities $n_0 + n$ and the filling factor $f_t = n_t/N_t$ of the bound-exciton states can be expressed as

$$n_0 + n = \frac{G - W_0\alpha - \beta + \sqrt{(G + W_0\alpha + \beta)^2 - 4\beta G}}{2W_0}, \tag{3}$$

$$n_t = f_t n_t = \frac{(n_0+n)N_t}{(n_0+n)+\alpha}\,, \tag{4}$$

where $\alpha = N_t(e_t + W_t)/c_t$ and $\beta = n_t W_t$. The physical meaning of the parameter α reflects the ability of trapping and emission of free excitons and free carriers from the excitonic traps. A small value of α means a high capture ability of the excitonic traps, while the parameter β reflects the maximum carrier recombination when the bound-exciton states are saturated.

There exist two extreme regimes in the current injection of a diode, which are determined by the magnitudes of the trap parameter α in the low- and the high-current regimes, i.e. $G \ll \alpha W_0$ and $G \gg \alpha W_0$, respectively:

$$n_0 + n \approx 0 \text{ and } f_t \approx \frac{n_0+n}{\alpha} \text{ for } G \ll \alpha W_0, \tag{5}$$

$$n_0 + n \approx \frac{G-\beta}{W_0} \text{ and } f_t \approx 1 \text{ for } G \gg \alpha W_0\,. \tag{6}$$

Equation (6) shows that the sum of the free-exciton and the free-carrier densities increases with the injection-current density after all the bound-exciton states are occupied by excitons. By extrapolating the linear part to $n_0 + n = 0$, we recognise the meaning of β, which is the minimum injection-current density required for saturating trap states. The thermal equilibrium between free carriers and free excitons connects the exciton system with the conductivity. Under a low-injection-current condition the carrier densities have a linear relationship with the free-exciton density as $n = c_0 n_0$. By replacing $n_0 + n$ with an expression for f_t and α in (4), the total series resistance R_s of the *pn* diode can be expressed as a function of the free-exciton density or the filling factor of the

bound-exciton states:

$$R_s = R_c + \frac{1}{e(\mu_e + \mu_h)(c_0 n_0 + n_{0b})} \tag{7}$$

or

$$R_s = R_c + \frac{1 - f_t}{e(\mu_e + \mu_h)\left[\left(\frac{c_0}{1+c_0}\alpha - n_{0b}\right) f_t + n_{0b}\right]}, \tag{8}$$

where $n_{0b} = (n_{e0}\mu_e + n_{h0}\mu_h)/(\mu_e + \mu_h)$; with n_{e0} and n_{h0} being the intrinsic free-electron and hole densities in the depletion region of the *pn* diode and μ_e, μ_h and e the mobility of electrons, holes and the electron charge, respectively. n_{0b} is basically the effective background free-carrier density determined by the doping in the p and n layers. Equation (8) shows that α is an important control parameter for the negative resistance in the semiconductor: for example, at low temperature, the series resistance R_c is smaller than the resistivity given by the background carriers $\sim 1/[e(\mu_e + \mu_h)n_{b0}]$. When the term $\alpha c_0/(1 + c_0)$ is larger than n_{b0}, a small change in f_t will result in a dramatic change of the second term of the right-hand side of (8). As f_t is varied from 0 to 1, the series resistance changes from a high stable value to a low stable value equal to the series contact resistance R_c. Therefore, a negative-resistance region will appear in a certain range of current density.

The *I–V* characteristics of a realistic *pn* diode usually are described by the general diode equation:

$$J = J_0\left[\exp\left(\frac{V - JR_s}{nkT}\right) - 1\right], \tag{9}$$

where J_0 is a constant, R_s is the series resistance and n is the ideality factor of the diode. From (3), (8) and (9) we can calculate the series resistance and the *I–V* characteristics of the diode. From these equations the negative differential resistance and bistability of the diode can be explained: from (9) we recognise that, for $0 < f_t < 1$, the state at a fixed voltage is unstable in a certain range of injection-current densities. Once a positive feedback is active for filling of bound-exciton states a change of the series resistance is induced by a small fluctuation of f_t. The current can jump to the upper branch or fall to the lower branch by positive feedback if a small fluctuation $dn_t/dt > 0$ or $dn_t/dt < 0$ is applied to the system. For example, when a fluctuation $dn_t/dt > 0$ occurs, bound excitons start to form by trapping free excitons as well as free carriers and the filling factor of bound excitons increases. This causes a decrease of the series resistance R_b in the negative differential resistance regime. At a fixed applied voltage, this will increase the junction voltage. Due to the nonlinear *I–V* relation of a *pn* junction (8), a slight increase of the junction voltage leads to a large increase of the injection of free carriers. In the case where the increase of the free-carrier densities due to the change of the junction voltage is larger than the carrier density, which is consumed by the formation of bound excitons, a positive feedback is built up. This results in a further increase of injection current and a further increase of f_t until all bound-exciton states are saturated. After the bound-exciton states are saturated, the free-exciton and carrier densities increase linearly with injection current and a strong decrease of R_b is expected. Finally, the current is limited by the constant series resistance to $I = V/R_c$. An opposite positive feedback process also occurs when a fluctuation $dn_t/dt < 0$ is added to the system and the current density is reduced below the value of β for sweeping down the voltage. The current will quickly fall to the low-current stable state in a voltage-controlled mode. Under the current-controlled mode, the decrease of resistance R_b due to the filling of the bound-exciton states will lead to a decrease of the overall applied voltage. Therefore, a negative differential resistance *I–V* curve is expected in the current range where the filling factor f_t of the bound-exciton states varies from a certain threshold value to 1.

In the presence of radiative recombination from free excitons and bound excitons, the electroluminescence (EL) intensities of free excitons and bound excitons are equal to the exciton density times the radiative recombination probability as $I_{FE} = W_{R0}n_0$ and $I_{BE} = W_{Rt}n_t$. The saturated bound-exciton luminescence intensity is $I_{SBE} = W_{Rt}n_t$. Considering that not all recombination processes of bound excitons are radiative and other unknown processes may influence the radiative transitions, we add a correction parameter γ to the α term for simulation of the EL of bound excitons as a function of current density. The luminescence intensities of free excitons and bound excitons are expressed as

$$I_{FE} = W_{R0}n_0 \cong \frac{W_{R0}}{1 + c_0}\frac{G - W_0\alpha - \beta + \sqrt{(G + W_0\alpha + \beta)^2 - 4\beta G}}{2W_0} \tag{10}$$

and

$$I_{BE} = W_{Rt}n_t = \frac{I_{SBE}(n_0 + n)}{\alpha\gamma + (n_0 + n)}. \tag{11}$$

Under steady-state conditions the luminescence intensity of the bound excitons is given as $I_{BE} = W_{Rt}n_t = I_{SBE}n_0/(\alpha + n_0)$. Due to the same dependence of the EL intensities as the exciton densities on the *I–V* characteristics of the diode, a bistability is also expected for the EL intensities from bound and free excitons.

3 Comparison of the rate-equation model to experimental results

The investigated Si *pn* diodes are prepared as follows: B^+ ions are implanted with a dose of 4×10^{15} cm^{-2} into n-type Si wafers with a resistivity of 0.1 Ω cm. The implantation is performed at 25-keV ion energy through a 50-nm thermally grown SiO_2 layer. Subsequent annealing is performed at 1050 °C for 20 min. Diodes with Al ring contacts of 1-mm diameter are lithographically prepared.

Figure 2a shows the EL spectrum of such a diode at a lattice temperature of 12 K under a forward current of 50 mA. At the lowest temperatures, three peaks can clearly be distinguished: P1 is the free-exciton line; P2 and P3 are two bound-exciton lines. The latter two are related to locally high boron densities in strain-free and strained environments, respectively. Detailed investigations of the physical origin of the two bound-exciton lines will be discussed elsewhere [31]. As shown in Fig. 2b, the intensity of P1 increases by two orders of magnitude at higher temperatures, while P2 decreases slightly. P3 has a higher binding energy and does not change its intensity in the temperature range shown.

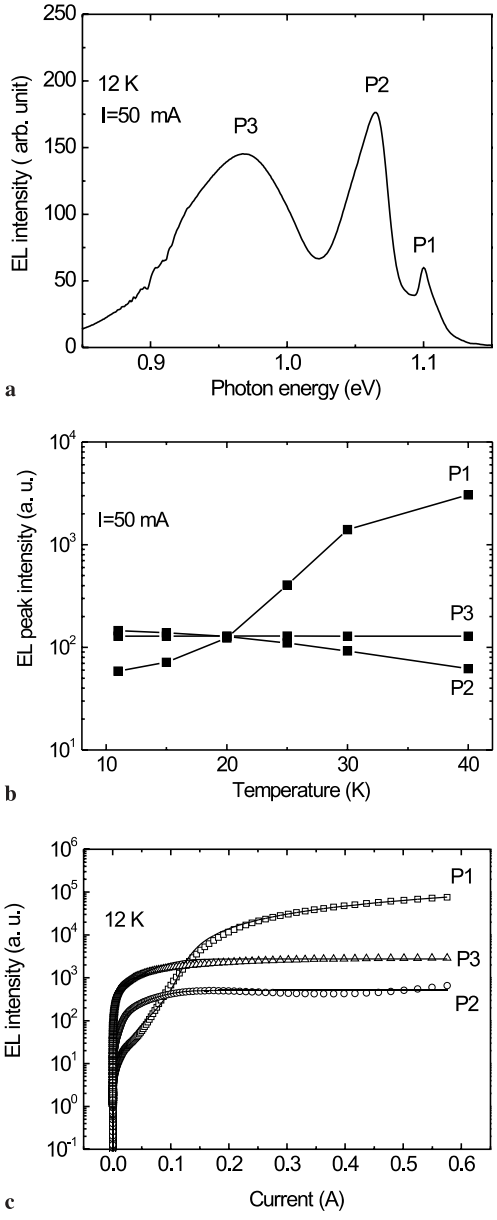

FIGURE 2 **a** EL spectrum of a Si *pn* diode at 50-mA current injection at a lattice temperature of 12 K. **b** Temperature dependence of the peak intensity of the three EL bands P1, P2 and P3. **c** EL output at the peak positions P1 (*squares*), P2 (*circles*) and P3 (*triangles*) as a function of the injection current at 12 K. The *solid lines* are results obtained from the numerical model

The intensity of the three lines is shown as a function of the injection current in Fig. 2c for 12 K lattice temperature. For low injection currents only the peaks P2 and P3 are present and their intensities rise with the injection current. For injection currents larger than 10 mA P1 starts to rise. At larger injection currents P2 and P3 saturate, while P1 further increases. The results of the numerical calculations are shown as solid lines and give a perfect agreement with the experiments. This shows that the population dynamics of the different excitonic levels/free carriers are well reproduced by the rate-equation model.

Figure 3 shows the *I–V* characteristics of the same diode in a current-controlled sweeping mode for different lattice temperatures. Up to temperatures of 30 K the *I–V* curves clearly

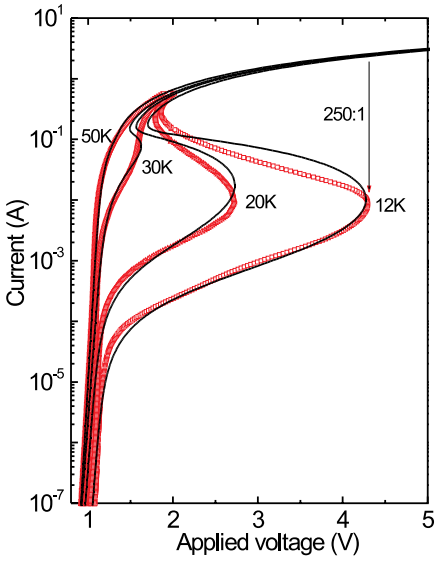

FIGURE 3 Current-controlled *I–V* curve of the Si *pn* diode at different lattice temperatures. The *scattered plots* are experimental data and the *solid lines* numerical calculations. The *arrow* indicates the maximum switching contrast between the bistable states of 250:1

exhibit an S-shaped behaviour, reflecting a strong negative differential resistance. This bistability is fully reproduced by the *I–V* curve calculated with the rate-equation model. The EL intensities of free and bound excitons exhibit the same bistable behaviour (not shown). As the temperature rises the thermal ionisation of the bound excitons as well as the background carrier density increases, thus leading to a quenching of the observed bistability.

For modelling the data, first the ideality factor n and J_0 in (9) are fitted for different temperatures from the current behaviour at small voltages (< 1.2 V). Then the current is calculated with the same set of parameters for all temperatures considering the temperature dependence of the background carrier concentration due to increased activation of dopants. It should be noted that the ideality factor used in the model is larger than 2, which indicates that the diode characteristics are dominated by recombination currents rather than diffusion currents (ideality factor of 1).

From the temperature dependence of the EL intensities (Fig. 2b) and the fit of the parameters of the rate-equation model to the temperature dependence of the bistability data, we derive a binding energy of 10 meV for the bound exciton P2 with the smaller binding energy. This is less than the energy difference of 35 meV between the FE luminescence bands P1 and P2. In comparison the binding energy of excitons bound to B in Si is 45 meV. This is an important hint towards the origin of the bound-exciton luminescence band P2, which we attribute to locally high boron concentrations leading to a three-dimensional potential variation similar to effects found in δ-doped semiconductors. The spatial extension of this potential variation is larger than that of a point defect, thus leading to the reduced binding energy.

4 Conclusion

We presented a rate-equation model which accounts for the carrier and exciton dynamics in Si *pn* diodes

prepared by ion implantation. The model is based on the dynamics of the population of bound excitons, free excitons and free carriers. The bistability observed in the current–voltage characteristics at low lattice temperatures and the temperature dependence of the electroluminescence are successfully described by the model. This underlines the relevance of bound excitons to the optical and electrical characteristics of Si devices. We note that the external quantum efficiency of the diodes investigated here is in the range of 0.1% at room temperature, which is close to the best reported values for diodes of this type [4]. The proposed model is useful for the description and further improvement of light-emitting Si *pn* diodes towards more efficient room-temperature operation.

REFERENCES

1 A. Forchel, P. Malinverni (eds.): *Technology Roadmap – Optoelectronic Interconnects for Integrated Circuits* (Office for Official Publications of the European Commission, Luxembourg 1998)
2 P.M. Fauchet: Mater. Res. Soc. Symp. Proc. **737**, F11.4.1 (2003)
3 L. Pavesi, L. Dal Negro, C. Mazzeloni, G. Franzo, F. Priolo: Nature **408**, 440 (2000)
4 W.L. Ng, M.D. Lourenco, R.M. Gwilliam, S. Ledain, G. Shao, K.P. Homewood, Nature **410**, 192 (2001)
5 M.A. Green, J. Zhao, A. Wang, P.J. Reece, M. Gal: Nature **412**, 805 (2001)
6 J. Zhao, M.A. Green, A. Wang: J. Appl. Phys. **92**, 2977 (2002)
7 F. Iacona, D. Pacifici, A. Irrera, M. Miritello, G. Franzo, F. Priolo, D. Sanfilippo, G. Di Stefano, P.G. Fallica: Appl. Phys. Lett. **81**, 3242 (2002)
8 L.T. Canham: Nature **408**, 411 (2000)
9 L.T. Canham: Appl. Phys. Lett. **57**, 1046 (1990)
10 V. Lehmann, U. Gösele: Appl. Phys. Lett. **58**, 856 (1991)
11 B. Gelloz, T. Nakagawa, N. Koshida: Appl. Phys. Lett. **73**, 2021 (1998)
12 S. Chan, P.M. Fauchet: Appl. Phys. Lett. **75**, 274 (1999)
13 L. Rebohle, J. von Borany, R.A. Yankov, W. Skorupa, I.E. Tyschenko, H. Fröb, K. Leo: Appl. Phys. Lett. **71**, 2809 (1997)
14 L. Rebohle, J. von Borany, H. Fröb, W. Skorupa: Appl. Phys. B **71**, 131 (2000)
15 G. Franzo, F. Priolo, S. Coffa, A. Polman, A. Carnera: Appl. Phys. Lett. **64** 2235 (1994)
16 B. Zheng, J. Michel, F.Y.G. Ren, L.C. Kimerling, D.C. Jacobson, J.M. Poate: Appl. Phys. Lett. **64**, 2842 (1994)
17 S. Coffa, G. Franzo, F. Priolo, A. Pacelli, A. Lacaita: Appl. Phys. Lett. **73**, 93 (1998)
18 C. Du, W.-X. Ni, K.B. Joelsson, G.V. Hansson: Appl. Phys. Lett. **71**, 1023 (1997)
19 J. Engvall, J. Olajos, H.G. Grimmeiss, H. Kibbel, H. Presting: Phys. Rev. B **51**, 2001 (1995)
20 T. Stoica, L. Vescam, M. Goryll: J. Appl. Phys. **83**, 3367 (1998)
21 T. Stoica, L. Vescan: Semicond. Sci. Technol. **18**, 409 (2003)
22 M. Stoffel, U. Denker, O.G. Schmidt: Appl. Phys. Lett. **82**, 3236 (2003)
23 E.Ö. Sveinbjörnsson, J. Weber: Appl. Phys. Lett. **69**, 2686 (1996)
24 J.M. Sun, T. Dekorsy, W. Skorupa, B. Schmidt, M. Helm: Appl. Phys. Lett. **82**, 2823 (2003)
25 M.A. Green: *Silicon Solar Cells: Advanced Principles and Practice* (Bridge Printery, Sydney 1995)
26 R. Corkish, D.S.-P. Chan, M.A. Green: J. Appl. Phys. **79**, 195 (1996)
27 D.E. Kane, R.M. Swansan: J. Appl. Phys. **73**, 1193 (1993)
28 P.L. Gourley, J.P. Wolfe: Phys. Rev. B **25**, 6338 (1982)
29 A. Dargys, S. Zurauskas: Semicond. Sci. Technol. **8**, 518 (1993)
30 X.Y. Zhang, K. Dou, Q. Hong, M. Balkanski: Phys. Rev. B **41**, 1376 (1990)
31 J.M. Sun, T. Dekorsy, W. Skorupa, B. Schmidt, A. Mücklich, M. Helm: unpublished